Effects of the Heat Transfer Fluid Selection on the Efficiency of a Hybrid Concentrated Photovoltaic and Thermal Collector

Catarina S. A. S. M. Campos

Instituto Superior Técnico, Lisbon, Portugal

Abstract—**This work focuses on the performance study of the PowerCollector™, a concentrated photovoltaic thermal system with a custom-made geometry and a photovoltaic cell cooling technology. To do so, a model that portrays the behavior of this concentrating solar system was developed. In order to validate all the information obtained with its simulation, measurements were taken from an experimental setup and were compared to the respective results predicted by this exact same model. It should be noted that all these procedures were based on the fluid for which PowerCollector™ has been designed (water). Hence, the efficiency enhancement by the use of nanofluids was also considered, as data from some studies addressing this issue were analyzed. Alongside all of this, the corrosion and erosion effects on the pipes incorporated in this system and originated by all the fluids mentioned throughout this investigation were also evaluated. In summary, with this entire study, it could be concluded that nanofluids may represent an appropriate alternative to water, as long as they are chosen according to all particularities of each case.**

Index Terms— **Corrosion, electrical and thermal efficiency, nanofluid, PowerCollector™.**

I. INTRODUCTION

OVER the years, with the ever-growing demand for power sources, solar energy generation has been gaining an increasing importance. It was with this mindset that a Swedish renewable energy company named SOLARUS developed the PowerCollector™, a concentrated photovoltaic and thermal (CPVT) collector with the potential to generate both electricity and heat [1]. Besides its outline, consisting of two identical halves with two solar panels each, this CPVT system also offers two main technologies with a great impact on its design: an Active Cell Cooling™ (ACC™) technology and a custom-made geometry called MaReCo™, which stands for Maximum Reflector Collector™. The latter, whose accurate classification for its shape is asymmetrical parabolic trough, is responsible for the sunlight concentration on the two-lower photovoltaic (PV) modules, whereas the former focuses on the heat extraction from the solar cells [1]. This cooling feature involves the use of a heat transfer fluid (HTF), which in turn plays a significant role in the thermal energy generation as well as in the electrical

efficiency of the PowerCollector™ [1]. The selection of different fluids as a cooling material is, therefore, expected to impose a significant impact on the efficiency of this exact same CPVT system, a subject matter worthy of a detailed analysis throughout this paper.

On a complementary note, it should also be pointed out that this paper is organized as follows: section I introduced in a brief manner the CPVT system configuration developed by SOLARUS and the problem under study. Section II addresses the methods and models used in a detailed way, so that a general idea of what was done is given and some notation is introduced. Section III evaluates the experimental results obtained using all the concepts mentioned in the previous section and also validates the developed model. Section IV, on the other hand, introduces and explains some novelties that might be beneficial to the efficiency of a CPVT system, namely in what concerns the heat transfer fluid. Section V concludes the paper.

II. THE POWERCOLLECTOR™ MODEL

As stated in the previous section of this paper, the SOLARUS PowerCollector™ is composed by several elements with a well-defined purpose and a very clear effect on its final yield. This means that, if one wants to develop an illustrating model of the different heat transfer fluid consequences on this system efficiency, it is recommended to divide it accordingly to its main features. Hence, the carried out design of the PowerCollector™ model for this particular study consists in a three-model implementation dependent on the results of each other, as described on the subsequent topics.

A. Optical Collector Model

One of the main features of this CPVT is the previously mentioned MaReCo™ technology, responsible for enabling all the concentrated sunlight reflection onto a limited area of the lower solar panels. Due to its unequable character with the sun's position, this area has a great influence on the amount of generated energy, which in turn means that the development of an optical collector model to determine the solar irradiance distribution throughout the day is an indispensable step to be taken. Consequently, every technical specification of the

system was taken into account and then transposed to SolTrace, a software tool dedicated to solar applications where the panel's tilt and its exact location are two parameters that need to be defined. Moreover, the local solar hour of the desired day to be simulated, based on the real motion of the sun and with the midday being on the moment it reaches the local meridian, is another important factor with a great impact on the concentrated sunlight distribution. In addition to all of this, with the resulting model it is also possible to observe a three-dimensional (3-D) representation of the modeled system with the solar rays' path for the imposed conditions (Figure 1).
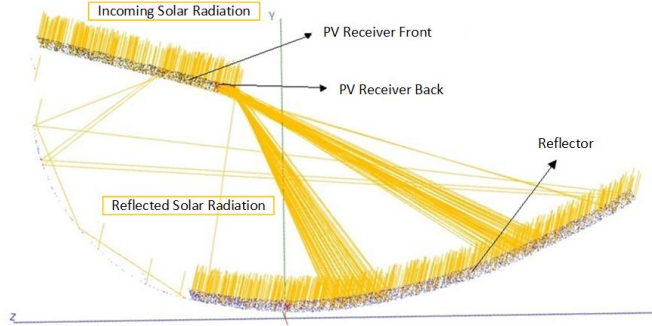

Figure 1 - 3-D representation of the optical collector model in SolTrace

B. Thermal Model

To estimate the thermal component behavior of this hybrid system it is necessary to model the total irradiance that reaches the PV modules, a procedure executed with COMSOL *Multiphysics®*. Furthermore, regarding the highly non-uniform performance of the received concentrated sunlight and according to all data acquired from the previously described model, the lower PV modules of the simulated CPVT were divided into three sections of uniform irradiance and adjustable width (Figure 2).
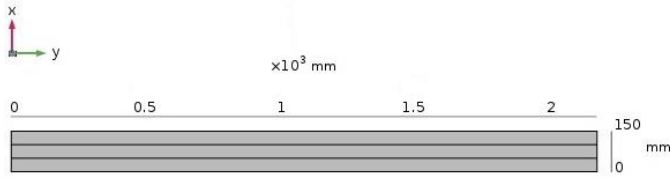

Figure 2 - Bottom view of the photovoltaic panel in COMSOL *Multiphysics®*

As for the physics behind the fluid flow on the designated tubes, this model needs to address the entire thermal phenomena related to the heat transferred to the fluid. Thus, it should be known that the thermal energy transmission between the receiving surfaces of solar radiation and the CPVT can be computed by the following equation [2],

$$\rho C_p \boldsymbol{u} \cdot \boldsymbol{\nabla} T = \boldsymbol{\nabla} \cdot (\kappa \boldsymbol{\nabla} T) + Q \qquad (1)$$

where ρ is the solid density in kg/m^3, C_p is the solid heat capacity at constant pressure in J/(kg·K), κ is the solid thermal conductivity in W/(m·K), $\boldsymbol{u}$ is the fluid velocity field in m/s, Q is the heat source in W/m^3, T is the collector's temperature in K and q is the heat flux in W/m^2. It is important to note that (1) describes the thermal conduction phenomena in a steady-state regime, which explains how the HTF extracts all the accumulated heat in the PV panels. The fluid motion, on the other hand, is mathematically depicted by both continuity and Navier-Stokes equations, which can be merged into a single expression for the steady-state regime [3],

$$0 = \boldsymbol{\nabla} \cdot \left[-p\boldsymbol{I} + \mu(\boldsymbol{\nabla}\boldsymbol{u} + (\boldsymbol{\nabla}\boldsymbol{u})^T) - \frac{2}{3}\mu(\boldsymbol{\nabla}\boldsymbol{u})\boldsymbol{I} \right] + \boldsymbol{F} \qquad (2)$$

In the previous equation, μ is the fluid's dynamic viscosity in Pa·s and p represents the fluid pressure in Pa. Additionally, for simplification purposes and considering the expected low fluid velocity, its flow was defined as being laminar.

Lastly, it is also important to include the collector's heat transfer with its surrounding environment performed through natural convection, a mechanism mathematically described as follows [2]:

$$-\boldsymbol{n} \cdot (-\kappa \boldsymbol{\nabla} T) = h(T_{amb} - T) \qquad (3)$$

As it can be seen from (3), the heat transfer coefficient, h, is a parameter that needs to be estimated, an assignment implemented with equation (4) [4]-[5],

$$\begin{cases} h = 4V_\infty + 5.6, \ V_\infty < 5 \ m/s \\ h = 7.1V_\infty^{0.78}, \ V_\infty > 5 \ m/s \end{cases} \qquad (4)$$

where V_∞ symbolizes the wind speed in m/s.

C. Electrical Model

The calculation of the collector's electrical performance is purely based on mathematical equations derived from the 3 parameters and 1 diode model (1M3P), a simplified model in which the non-linear solar cell's *I-V* (current-voltage) characteristic can be both obtained and explained with an equivalent electric circuit. Regarding this curve, it is possible to underscore the current and voltage values for which the peak power (I_{MP} and U_{MP}, respectively) is obtained, which basically consists of ascertaining the point where the power produced by the cell is maximum. This point's designation is, therefore, Maximum Power Point (MPP) and its value varies with changing atmospheric conditions such as irradiance and ambient temperature. The method used by the 1M3P model to acknowledge this issue is based on the definition of several parameters, whose value depends on these two meteorological characteristics. Both I_{MP} and U_{MP} are then computed using these exact same quantities, resulting in a peak power value also variable with the irradiance and ambient temperature [6],

$$P = U_{MP} \cdot I_{MP} \qquad (5)$$

Given that MPP represents the operating point where the PowerCollector™ should always be working on, the previous equation represents the desired value for the electrical power generated. The required irradiance and temperature values to compute it were obtained from the previously mentioned thermal and optical collector models.

1) Influence of Temperature

Solar cells become less efficient as they heat up, an effect that clearly has repercussions on the electricity generation of the system. In the 1M3P model, one of the main parameters that

expresses this temperature dependence is the thermal voltage (V_T), a value used for most of the remaining quantities' computation [6],

$$V_T = \frac{KT}{q} \qquad (6)$$

and whose equation shows a variation with the Boltzmann constant, K, which is 1.38×10^{-23} J/K, the cell's temperature, T in K, and the electron charge, q, of 1.6×10^{-19} C. Nevertheless, when it comes to the electrical influence of the photovoltaic cell's temperature, the diode's reverse saturation current (I_0) also plays an important role, with its equation being dependent on both V_T and T [6],

$$I_0 = I_0^r \left(\frac{T}{T^r}\right)^3 \exp\left[\frac{\varepsilon \cdot N_S}{m}\left(\frac{1}{V_T^r} - \frac{1}{V_T}\right)\right] \qquad (7)$$

In the previous equation, the upper index r represents a standard test condition (STC) parameter, ε is the band gap (1.12 eV for silicon), m is the diode's ideality factor and N_S is the number of cells in series.

2) Influence of Irradiance

Considering the solar cell's operating principle, it should be foreseeable an increase in the generated electrical power with the harnessing of more solar radiation. The short-circuit current (I_{SC}) is the parameter that intends to describe this exact same effect on the cell's performance with the following equation [6],

$$I_{sc} = \frac{G}{G^r} I_{sc}^r \qquad (8)$$

where G corresponds to the irradiance reaching the solar cells in W/m^2.

3) Constant Parameter and Final Computations

Lastly, there is also another important parameter that does not depend on any atmospheric condition, the diode's ideality factor (m). In fact, its calculation requires the use of only values given in the manufacturer datasheet, as it can be seen from (9) [6],

$$m = \frac{U_{MP}^r - U_{OC}^r}{V_T^r \ln\left(1 - \frac{I_{MP}^r}{I_{sc}^r}\right)} \qquad (9)$$

Once all these calculations are concluded, the desired computation of I_{MP} and U_{MP} can finally occur with the use of the following pair of equations [6]:

$$\begin{cases} U_{MP}^{(k+1)} = mV_T \ln\left(\frac{\frac{I_{sc}}{I_0}+1}{\frac{U_{MP}^k}{mV_T}+1}\right) \\ I_{MP} = I_{sc} - I_0(e^{\frac{U_{MP}}{mV_T}} - 1) \end{cases} \qquad (10)$$

As the U_{MP} equation is non-linear, its resolution should be done with an iterative method where U_{MP}^r is the reference value.

III. VALIDATION OF THE MODEL

To validate the developed model, a set of experiments were performed on an actual PowerCollector™ installed on the Taguspark terrace. The main goal of the experimental tests was to measure the CPVT's electrical performance throughout a summer day in which the PV modules were either cooled or non-cooled. The comparison between all the obtained data and the respective results predicted by the model will determine how well this exact same model is able to depict an actual PowerCollector ™ setup.

In this case, besides the already defined CPVT location, there are also some other parameters that must be carefully chosen to get the most out of the photovoltaic system to be installed. The collector's orientation and the solar panel's tilt, for instance, are two elements with an extreme importance to any solar system efficiency. In Portugal, considering the results of some studies carried out over the years, solar panels facing south is the most common alternative used and, based on this, the chosen orientation for the future setup was also south [6]. Furthermore, to choose the best tilt for the desired configuration, an in-depth study of the absorbed solar power variation with this parameter was estimated for every month of the year. With all the obtained data, an attempt was made to choose a value at which the concentration effect is boosted throughout the year and, after some analysis, that value was found to be 15º.

For the thermal installation, a hose with a water flow of 0.5 m^3/h was connected to one of the halves of the system, whereas the other half received the cooling fluid through a connecting thermal fitting. In relation to the electrical installation (Figure 3), the two halves were connected in series and the output current and voltage were measured using an ammeter and multimeter, respectively. The connection between the collector and the grid was done with a Maximum Power Point Tracker (MPPT), a device responsible for the desired MPP operation. Moreover, a pyranometer and a temperature sensor were also used on the experiments to measure the actual irradiance reaching the upper PV modules and the ambient temperature, respectively.
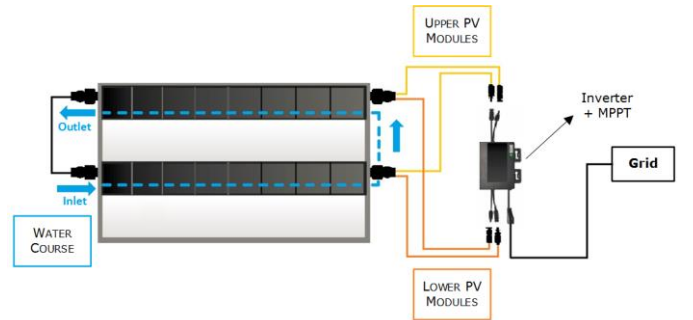

Figure 3 - Schematics of the PowerCollector™ electrical installation

With this setup, two experimental tests were done in an alternating manner. On the first one, voltage and current measurements were carried out on specific hours of the day without any PV cell cooling. On the second one, however, an extra temperature sensor was used to measure the outlet and inlet fluid's temperature, meaning that in this case the exact same procedure was executed but with the ACC™ technology also included.

A. Experimental Results

From the acquired voltage and current values, the electrical power produced by the panels was determined for the exact

moment all the previously mentioned measurements were collected. A wattmeter included in the setup also registered this parameter's evolution throughout the entire experiment (Figure 4).
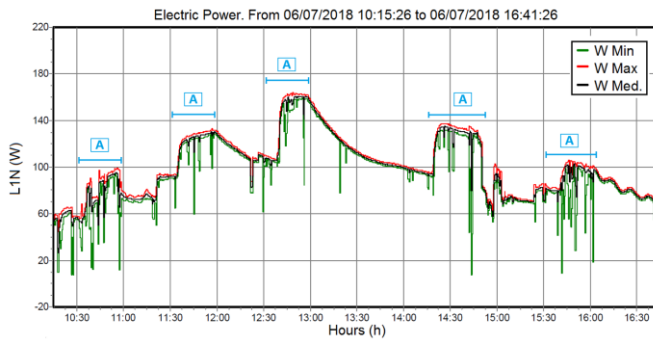

Figure 4 - Electric power evolution obtained throughout the entire experiment. Cooling of the PowerCollector™ panels indicated in A.

As it can be seen from Figure 4, at specific moments of the day, there are some abrupt changes on the generated power. The reason for this is related to the HTF flow, which has a positive impact every time it is incorporated to the system and a negative one when the fluid stops flowing through the cooling tubes.
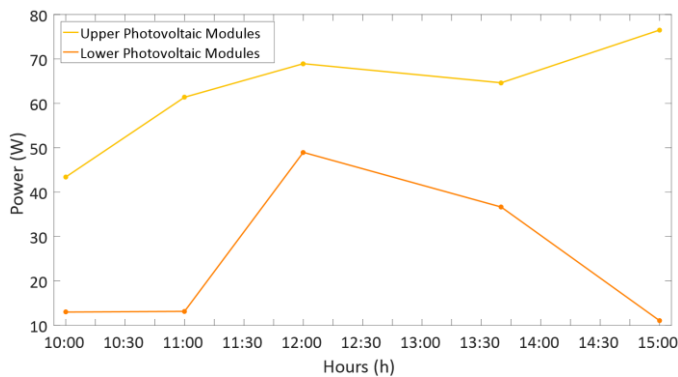

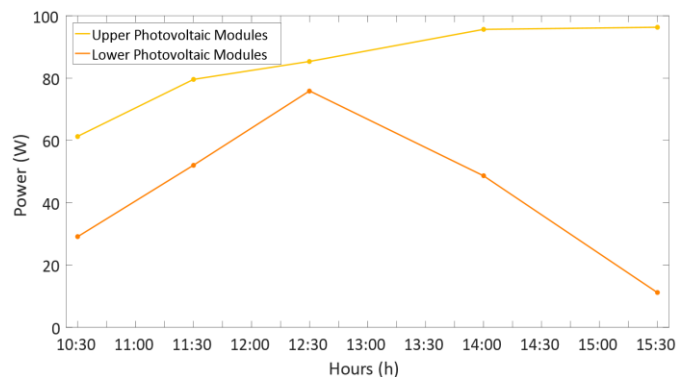Figure 5 - Electric power produced by each PowerCollector™ panel in the non-cooling experiment

Figure 6 - Electric power produced by each PowerCollector™ panel in the cooling experiment

Even though the concentration factor is less than 1, the obtained results for both experimental tests (with and without the cooling technology, depicted in Figure 6 and Figure 5, respectively) show the concentration effect on the lower PV

modules and also demonstrate the clear improvement on the efficiency values when all the cells are cooled down.
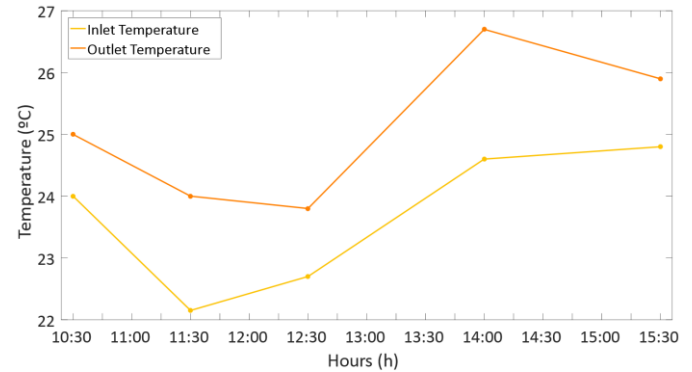

Figure 7 - Inlet and outlet temperature of the water

The small difference between the fluid's initial and final temperature should also be mentioned, because that is only possible on a steady-state regime, simulated during the experiment with the purpose of obtaining experimental results (Figure 7) as close as possible to the predicted ones.

B. PowerCollector™ Positioning Correction

As stated before, after the experimental tests, the exact same conditions were simulated using the PowerCollector™ model, so that all the results obtained could then be compared. However, as it can be seen by the results on and Table 2, when that was done the error between the predicted and experimental results was slightly higher than expected, namely for the lower PV modules' power values (P_{low}, with a maximum error of 44.8%). Conversely, the error for the power produced by the upper solar panels (P_{up}) was considered to be relatively low, as it was less than 15%. The same can be said about the difference between the fluid's inlet and outlet temperature (ΔT), whose error was only about 1%.

Table 1 - Results obtained by the developed PowerCollector™ model for the non-cooling experiment

Hours	Model Results		Error	
	P_{up} [W]	P_{low} [W]	P_{up} [%]	P_{low} [%]
10:00	46.91	0		
11:00	56.89	0.59		
12:00	58.09	26.12	14.07	23.19
13:40	47.07	62.07		
15:00	53.43	45.64		

Table 2 - Results obtained by the developed PowerCollector™ model for the cooling experiment

Hours	Model Results			Error		
	P_{up} [W]	P_{low} [W]	ΔT [ºC]	P_{up} [%]	P_{low} [%]	ΔT [%]
10:30	54.01	0.34	0.42			
11:30	70.70	1.64	0.16			
12:30	78.98	57.80	0.87	13.2	44.8	0.82
14:00	78.63	107.20	1.76			
15:30	76.05	65.18	1.24			

The main reason for this discrepancy is related to the difference between the collector's concentration effect predicted by the simulated model and the one actually observed. By analyzing and comparing all the available data, it was concluded that the potential problem causing this inconsistency was the defined orientation of the PowerCollector™ in its model. Hence, in order to demonstrate this theory, some simulations regarding the CPVT orientation were done by changing the initial value used on the optical collector model ($\zeta = 90°$) by 5%. On a complementary note, the effects on the concentrated sunlight induced by the panel's tilt (θ) were also considered. According to the obtained results (Figure 8 and Figure 9), even though the tilt variation does not influence the displacement of the concentration effect on the PV receiver's back, the orientation (ζ) on the other hand, has a significant impact on this exact same aspect.
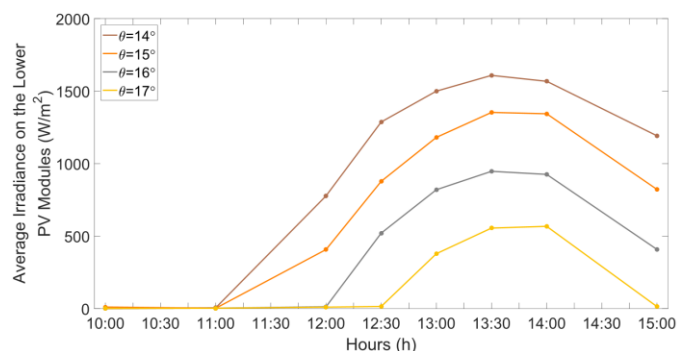

Figure 8 - Variation of the average irradiance on the lower PV modules with its tilt
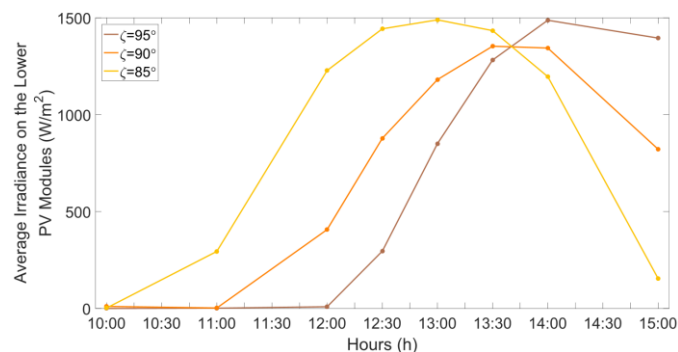

Figure 9 - Variation of the average irradiance on the lower PV modules with its orientation

Knowing that the power produced by the lower panels is directly dependent on the incoming irradiance, when one compares the curves from Figure 8 and Figure 9 with the correspondent experimental values presented in Figure 5 and Figure 6, a greater similarity between the experimental data and the values for the curve in which $\zeta = 85°$ was found. Following the same reasoning as before, the CPVT model was once again used to simulate its behavior with the new orientation value. As it can be seen from Table 3 and Table 4, the enhancement on both P_{low} errors is clear when compared to the ones presented on   and Table 2. Moreover, the remaining error values for the other parameters (ΔT and P_{up}) are still relatively low. Based on this, it can be declared that the real Powercollector™ orientation is not exactly the one initially planned (south).

Table 3 - Results obtained by the developed PowerCollector™ model for the non-cooling experiment with the new orientation value

Hours	Model Results		Error	
	P_{up} [W]	P_{low} [W]	P_{up} [%]	P_{low} [%]
10:00	46.89	0.19		
11:00	52.81	26.29		
12:00	45.40	65.87	15.4	16.6
13:40	46.06	63.96		
15:00	62.45	13.42		

Table 4 - Results obtained by the developed PowerCollector™ model for the cooling experiment with the new orientation value

Hours	Model Results			Error		
	P_{up} [W]	P_{low} [W]	ΔT [ºC]	P_{up} [%]	P_{low} [%]	ΔT [%]
10:30	51.52	0.72	0.41			
11:30	70.37	71.55	1.77			
12:30	78.56	115.7	1.06	13.5	31.3	0.33
14:00	78.69	93.67	2.08			
15:30	76.31	1.18	0.67			

Further conclusions can be drawn from the analysis of all these data. Regarding the panel's tilt, for instance, there is a possibility that the mounted PowerCollector™ on Taguspark has a slightly higher value for θ than 15º because of the lower average irradiance that is expected to reach the back of the PV receiver for higher values of θ (Figure 8), which is closer to the obtained experimental results (Figure 5 and Figure 6). However, it should also be taken into account the inability of SolTrace to compute the diffuse radiation reaching the solar panels. Notwithstanding all this, according to the overall results, the CPVT model is validated.

IV. EFFECTS OF USING ALTERNATIVE HEAT TRANSFER FLUIDS

After the operation analysis of the SOLARUS' CPVT in the Taguspark terrace, the next step consists on the investigation of the hypothesis of using a further heat transfer fluid other than water. The reason behind this fluid as a first choice is related to the fact that the PowerCollector™ cooling system was originally designed to operate with water, which is a very common situation for most solar thermal systems these days [7]. Its high heat capacity at constant pressure (C_p) as well as its low cost are the main reasons for this. However, as the demand for CPVT systems increases, the enhancement of this systems' performance becomes a very important subject to be studied. In order to achieve this goal, one of the hypotheses currently under study is the use of nanofluids, as they have augmented thermal conductivities and a C_p close to that of water, which means that their use is expected to be very beneficial for both thermal and electrical efficiency of any CPVT system. The real consequences of this type of fluids use is, therefore, something that needs to be studied, especially when it comes to the system global efficiency and possible corrosion and erosion effects.

A. Global Efficiency

The first step to evaluate the feasibility of the nanofluids use is related to the realization of simulations that demonstrate the potential of these fluids in terms of the efficiency of CPVT systems. In [8], for instance, an Al_2O_3-water nanofluid was simulated using a two-dimensional (2-D) model of a CPVT system similar to the PowerCollector™ so that the thermal and electrical energy generated could be estimated. The obtained results were then compared to the ones for the exact same system but with water as a HTF (Figure 10).
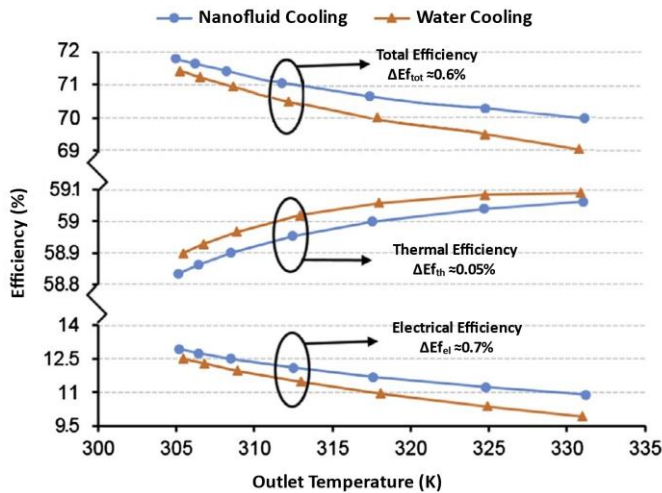

Figure 10 - Evolution of the CPVT efficiency as a function of the outlet temperature of the two heat transfer fluids under study (adapted from [8])

Even though results show how the thermal conductivity for nanofluids can improve the electrical energy generation ($\Delta Ef_{el} \approx 0.7\%$), the same cannot be said about the thermal efficiency that, in addition to its value decrease, has a very small variation in comparison to the results of the water simulation ($\Delta Ef_{th} \approx 0.05\%$). This can be explained with the small difference between the nanofluid's heat capacity at a constant pressure (approximately 4.212 kJ/kg/K) and the water C_p (approximately 4.22 kJ/kg/K). However, it should be noted that this decrease is clearly less significant than the electrical efficiency enhancement, which makes the system global efficiency slightly higher when a nanofluid is used ($\Delta Ef_{tot} \approx 0.6\%$). Thus, with this study it can be concluded that, in the long-run, a nanofluid-based system is preferable to a water-based one. Nonetheless, there are also other factors that are worth evaluating, like for example the deterioration of the tubes through which the nanofluid flows.

B. Corrosion and Erosion

In order to evaluate the corrosion effect on metal surfaces, as the aluminium of the PowerCollector™ cooling tubes, in [9] and [10] some experiments were carried out to determine which factors have a greater influence on this metal degradation effect. In both studies, each nanofluid had water as its base fluid and the nanoparticles varied between Al_2O_3, TiO_2 and SiC. In the particular case of [9], all the aluminium sample targets used

were exposed to similar operating conditions (fluid flow between 5 and 6 m/s and temperature ranging from 20ºC to 25ºC) during a certain period of time (2 to 3 weeks).

Table 5 - Summary of the experimental results obtained for the aluminium sample targets [9], [10]

Nanofluid	Observed Results Description	pH
Al_2O_3 – 9%	High deterioration effect, with 182 μm decrease in thickness of the area exposed to the fluid.	8.8
Al_2O_3 – 3%	Very strong corrosion effect and considerable decrease in the sample targets thickness (263 μm).	8.6
TiO_2 – 9%	Damaging similar to the water. Incrustation of nanoparticles deposit.	7.3
SiC – 3%	No significant corrosion effects when compared to water.	5.9

According to all the data provided in Table 5, the aluminium corrosion and erosion effects appear to be rather complex, since there are completely different results for each of the particles that make up the nanofluids under study. These results suggest that, unlike what was to be expected, the nanoparticles present in the nanofluid do not have a major influence on the aluminium erosion. The nanofluid's pH, on the other hand, seems to be the key to understand the reason behind the results described in Table 5. As a passive metal, aluminium has a very high corrosion resistance, which is the result of a natural protective oxide film formation immediately after first exposure to air or water [11]. Hence, provided that the pH of the fluid which is in contact with the aluminium is comprised between this protective layer's stability limits (approximately between 4 and 9), the degradation effects on this metal will definitely be minimized [12]. To prove this assumption right, in [10] an experiment where the nanofluid with a pH closer to the previously mentioned stability limits (Al_2O_3 – 9%) is modified so as to have a lower pH (6.5). The results of this experiment show a significative decrease in the erosion rate of the aluminium, which is 79.7 for the case of the nanofluid with the lowest pH and 264 for the initial situation described in [9]. Bearing in mind that, the main deterioration effects observed in the aluminium when the fluid used on the PowerCollector™ is water is caused by pitting corrosion [13], it can be stated that in any of the choices there will be some degradation of this metal and depending on the nanofluid used, there can either exist advantages in using nanofluids or not.

V. CONCLUSION

The importance of studying the principle of operation of hybrid solar systems such as the PowerCollector™ is based on the need to fully understand all its features and specifications before considering any type of optimization. For this purpose, a model that portrays both thermal and electrical behavior of this system was developed and experimentally validated. Factors such as the PV modules' tilt and orientation show a very visible effect on the amount of concentrated sunlight, which in turn proves the importance of a previous study about all the possible options for any photovoltaic setup. In the case of the one installed on Taguspark, it could be concluded that the tilt

which would boost the amount of electrical power throughout the year would be 15º. As for the cooling system of the PowerCollector™, comparing the obtained results for both sets of measurements (with and without the cooling technology), the advantages of including this feature are clear, since that under the conditions studied, there always seems to be a difference of about 20W for the generated electrical power. The chosen fluid to do all these experiments was water, the Heat Transfer Fluid for which the PowerCollector™ cooling system was originally designed to operate with. The feasibility evaluation, in terms of energy conversion efficiencies, of using other fluids other than water in a CPVT system was then included. Initially an Al_2O_3-water nanofluid showed an improvement in electrical and total efficiencies, whereas the thermal efficiency slightly decreases. This demonstrates an overall efficiency enhancement in the long-run. Further studies were considered to analyze possible corrosion and erosion effects on aluminium, the PowerCollector™ cooling tubes material, due to the use of several nanofluids. A careful analysis of the data showed that the main cause for this metal deterioration is due to chemical corrosion caused by the fluid's pH rather than mechanical erosion by the nanofluid's solid particles. All in all, it can be concluded that it is possible to use a nanofluid in the PowerCollector™ and obtain better efficiency results than water. However, before any decision, there must be a previous investigation to understand which advantages and disadvantages each possible nanofluid might bring.

REFERENCES

[1] SOLARUS, "Brochure", p.8-11, 2017. [Online] Available at: https://solarus.com/powercollector/. [Accessed 12 March 2018].

[2] COMSOL, "Heat Transfer Module User's Guide", Chapter 6, p.431-465, 2017.

[3] COMSOL. "COMSOL Multiphysics Reference Manual", Chapter 13, p. 782-786, 2017.

[4] Thijs Defraeye, Bert Blocken, Jan Carmeliet, "Convective heat transfer coefficients for exterior building surfaces: Existing correlations and CFD modelling", *Energy Conversion and Management*, Volume 52, Issue 1, p. 512-522, 2011.

[5] B. Blocken, T. Defraeye, D. Derome, J. Carmeliet, "High-resolution CFD simulations for forced convective heat transfer coefficients at the facade of a low-rise building", *Building and Environment*, Volume 44, Issue 12, p. 2396-2412, 2009.

[6] Rui Castro, "Uma introdução às energias renováveis: eólica, fotovoltaica e mini-hídrica", *IST Press*, Issue 2, 2011.

[7] Jee Joe Michael, Iniyan S, Ranko Goic, "Flat plate solar photovoltaic–thermal (PV/T) systems: A reference guide", *Renewable and Sustainable Energy Reviews*, Volume 51, p. 62-88, 2015.

[8] Zelin Xu, Clement Kleinstreuer, "Concentration photovoltaic–thermal energy co-generation system using nanofluids for cooling and heating", *Energy Conversion and Management*, Volume 87, p. 504-512, 2014.

[9] Gian Piero Celata, Francesco D'Annibale, Andrea Mariani, Salvatore Sau, Emanuele Serra, Roberto Bubbico, Carla Menale, Heiko Poth, "Experimental results of nanofluids flow effects on metal surfaces", *Chemical Engineering Research and Design*, Volume 92, Issue 9, p. 1616-1628, 2014.

[10] Roberto Bubbico, Gian Piero Celata, Francesco D'Annibale, Barbara Mazzarotta, Carla Menale, "Experimental analysis of corrosion and erosion phenomena on metal surfaces by nanofluids", *Chemical Engineering Research and Design*, Volume 104, p. 605-614, 2015.

[11] Mengxia Liang, Robert Melchers, Igor Chaves, "Corrosion and pitting of 6060 series aluminium after 2 years exposure in seawater splash, tidal and immersion zones", *Corrosion Science*, Volume 140, p. 286-296, 2018.

[12] Ph. Gimenez, J.J. Rameau, M. C. Reboul, "Experimental pH potential diagram of aluminium for sea water", *Corrosion*, Volume 37, p. 673-681, 1981.

[13] Christian Vargel, "Corrosion of Aluminium", Elsevier, 2004.